

REACTIVE WETTING IN CORROSION: A MILD STEEL EXAMPLE

L. W. Ng¹, C. Fung², J. N. Connor², Y. Ngothai¹, D. Druskovich³ & R. Sedev²

¹School of Chemical Engineering, University of Adelaide, Adelaide, South Australia, ²Ian Wark Research Institute, University of South Australia, South Australia & ³Science Engineering and Health, CQUniversity Australia, Queensland

SUMMARY: Wettability is a key factor in various engineering, scientific and industrial processes. The contact angle is the most common measure of the degree to which a liquid wets a solid surface. However, most investigations of contact angles focus on rather ideal systems where liquids wet inert, smooth, and homogeneous surfaces which rarely exist in the real world. Reactive wetting occurs when the liquid reacts with the solid (as in corrosion) and has received much less attention. While the wetting principles remain unchanged, in time the chemical reactions affect the composition and properties of the three-phase system. The influence of chemical kinetics is further complicated by the effects of mass transport. We have examined the corrosion of mild steel under a small aqueous droplet (basic, neutral or acidic). In order to correlate the corrosion process with the wettability of the metal surface, electrochemical measurements of the corrosion rate were combined with contact angle measurements. We show how wettability is affected by corrosion and, at the same time, the local corrosion rate is modified by the conditions imposed by the fixed volume of the droplet and its evaporation. These findings are relevant for the performance of tools and engineering structures subjected to water spraying or under condensation-evaporation conditions.

Keywords: Corrosion, Contact angle, Reactive wetting, Mild steel

1. INTRODUCTION

Wetting is an important phenomenon and is widely studied and used in engineering, scientific and industrial processes. The contact angle is a measure of the wetting of a solid by a liquid in ambient vapour or an immiscible second liquid. It is an important parameter in material performance and engineering design. A vast amount of literature exists on the contact angles in solid-liquid-vapour systems. However, most investigations have concentrated on rather ideal systems where liquids are placed on rather smooth and homogeneous surfaces. In addition to that, most liquids and solids investigated are inert. In practice such ideal behaviour is rare as most solid surfaces are heterogeneous and rough and chemical reactions between the solid and the liquid are possible. Reactive wetting occurs in systems where the liquid reacts with the solid. These systems are complex since the wettability may change in time due to diffusion, oxidation, reduction and evaporation.

One important occurrence of reactive wetting in industries as well as daily life is the corrosion of metal due to aqueous electrolyte droplets sitting on its surface. The corrosion rate increases with an improved wetting of the solid surface (i.e. smaller contact angle) since the contact area between the metal and the liquid is larger. The wetting behaviour of typical reactive three-phase systems would be affected by the corrosion reaction. This research is aimed at gaining some understanding of the effects of corrosion on the wetting of aqueous electrolyte droplets sitting on metal surfaces.

In this study, we correlate the wettability of aqueous droplets on mild steel with the corrosion rate of the metal. Three aqueous droplets (0.5 M H₂SO₄, 0.5 M NaOH, and 0.6 M NaCl) were used to vary the corrosion rate of mild steel. The corrosion rate was measured using the potentiodynamic linear polarisation resistance method. The active-passive behaviour of mild steel was characterised with potentiodynamic anodic polarisation curves. In a separate experiment the wettability of steel was characterised by measuring the contact angle with the sessile drop technique. Finally, the surface of mild steel was examined (before and after corrosion) using a scanning electron microscope and low power optical microscopy to characterise the effect of corrosion on the surface.

1.1 Wetting and contact angles

Wettability is defined as the tendency for a liquid to spread on a solid substrate in vapours or in an immiscible liquid. The degree of wetting is indicated by the contact angle formed at the solid-liquid interface which depends on the interfacial

energies (Adamson & Gast, 1997). Wetting involves a balance between the interfacial tensions and the adhesion between the liquid-solid phases. Its equilibrium behaviour is described by Young's equation.

When a drop of liquid is placed on a solid surface, the drop spreads until it reaches a constant shape as shown in Figure 1.

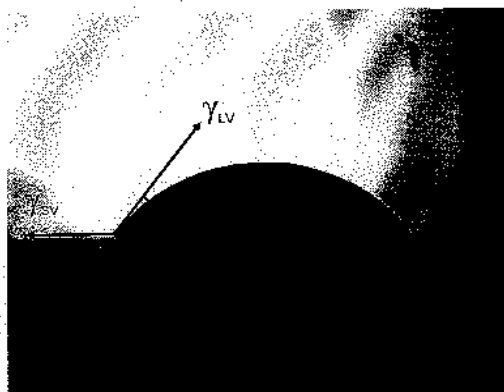


Figure 1 A drop of NaCl on a polished mild steel surface, showing the interfacial tensions.

The angle between the liquid-vapour and solid surfaces, θ , is called contact angle. The contact angle is determined by the three interfacial tensions γ_{SV} , γ_{SL} and γ_{LV} (S, L and V denote the solid, liquid and vapour phases, respectively). When the three interfacial tensions are in equilibrium, they are related by Young's equation (Adamson & Gast, 1997):

$$\gamma_{SV} - \gamma_{SL} = \gamma_{LV} \cos \theta. \quad (1)$$

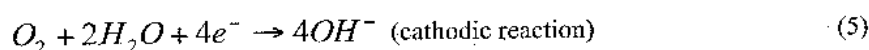
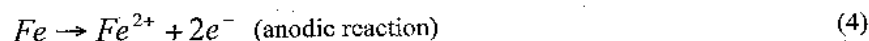
The contact angle described by Young's equation is the equilibrium contact angle. In practice a variety of static contact angle values are measured. This hysteric range is bound by the advancing and receding contact angles. The advancing contact angle is usually more reproducible and considered more relevant to the energetics of the solid surface.

1.1.1 Reactive wetting

In reactive wetting, wetting is influenced by chemical reactions between the spreading liquid and the solid substrate (Girish & Narayan, 2007). In the case of metal corrosion, corrosion products are formed at cathodic areas while dissolution occurs at anodic areas. Since chemical reactions occur at the interface between the solid and the liquid, the interfacial tension γ_{SL} changes and that affects the contact angle. The migration of corrosion products may further complicate the situation. There have been a limited number of studies, e.g. those by Muster et al. (2004, 2005) where the relationship between corrosion rate and the wettability of aqueous drops have been examined. However, a major part of the research efforts has been directed toward the study of reactive wetting of molten metals on a variety of surfaces (Eustathopoulos et al, 1999). The changes in the interfacial energies of the system were related to the interfacial reactions. It was found that the steady-state contact angle on the parent surface is almost identical to the contact angle obtained on the reaction product itself. Based on these observations, Eustathopoulos et al (1999) proposed the Reaction Product Control (RPC) model to describe reactive wetting. This model states that the final degree of wetting in reactive systems is controlled by the product formed at the interface and not by the parent material.

1.2 Corrosion of iron in oxygenated solutions

The corrosion and passivation of mild steel in NaOH, NaCl, and H₂SO₄, and have been studied extensively (Lyon, 2010). When mild steel comes in contact with an aqueous droplet, the oxidation and reduction reactions are as follows:



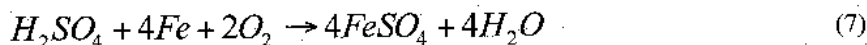
or/and



The cathodic reaction depends on the pH of the aqueous solution.

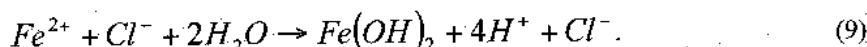
Higher corrosion rates are expected when mild steel is contacted with H₂SO₄, although the actual rate is concentration dependant (Panossian et al., 2012). In a strong acid (e.g. sulphuric acid) the dissolution of Fe to Fe²⁺ ions is accelerated due

to increased evolution of H_2 from H^+ at the cathode. According to Ahmad (2006), in oxygenated systems, the net reaction involving sulphuric acid and mild steel can be described by



When steel is in contact with NaOH, the metal passivates and the corrosion rate drops. According to Jovancicevic et al. (1986), the passive layer consists of a thin film of crystalline Fe_2O_3 with various water content. Freire et al (2008) reported that, under alkaline conditions, the passivating film is inhomogeneous and contains Fe^{2+} and Fe^{3+} oxides and hydroxides.

Pitting corrosion of mild steel is expected in the presence of NaCl and H_2SO_4 due to the presence of the Cl^- and SO_4^{2-} ions which lead to the breakdown of the passivation layer and also interfere with its reformation. For mild steel in a well oxygenated NaCl solution of pH between 4 and 8 the anodic and cathodic reactions are given by equations 4 and 5. Due to the dissolution of Fe, an excess of positive metal ions, Fe^{2+} , accumulates within the pit. To maintain charge neutrality, Cl^- anions from the electrolyte will migrate into the pit where the following hydrolysis reaction occurs:



The presence of H^+ and Cl^- ions prevents the self-repassivation of the metal as well as increases the pH within the pit. This increases the dissolution of the metal which increases the formation of Fe^{2+} and Cl^- which in turn generates more H^+ and Cl^- through hydrolysis (Ahmad, 2006). Thus, the pitting process is autocatalytic and the pitting rate increases in time.

1.3 Corrosion under droplets

Corrosion under droplets is complicated by the geometry of the liquid drops. On one hand, corrosion is patchy as the conditions under the droplet are different from the metal exposed in between the droplets. On the other hand, the restricted volume of the liquid allows for aeration to be more significant in the surface layer. As a consequence the corrosion conditions under the droplets are uneven: less oxygen in the middle and more oxygen near the periphery. As a result, local corrosion develops: an anodic region in the middle and a cathodic region near the solid-liquid border. Evans introduced the concept of aeration differential cells and demonstrated the variation in pH across the base area of a corrosive droplet (Landolt, 2007). The problem is relevant to atmospheric corrosion and situations involving dry-wet cycles, and has attracted increasing attention in recent years (Dubuisson et al 2006, Dubuisson et al 2007, Hastuty et al, 2010, King et al, 2011, Muster et al, 2011, Li and Hihara, 2012).

2. METHODOLOGY

2.1 Reagent Preparation

Experiments were conducted using three aqueous solutions: 0.50 M H_2SO_4 , 0.50 M NaOH and 3.5 wt% (0.61 M) NaCl. Solutions were prepared from AR grade NaOH pellets and AR grade NaCl crystals, respectively, both supplied by Merck. A 0.5 M H_2SO_4 was obtained by dilution of 30% H_2SO_4 (Chem-supply). Milli-Q water was used to prepare all solutions.

2.2 Preparation of the mild steel samples

Three samples were machined from a cylindrical 1020 mild steel rod (1 cm diameter). The steel samples were rinsed with acetone and dried with nitrogen gas before being cast in epoxy resin. Once the epoxy had completely set, the top and base of the casts were machined flat. A hole was drilled and tapped in the base of each cast so that a small spring could be inserted in the hole to provide electrical contact with the metal sample and a protruding metal screw during corrosion measurements.

To ensure the surface was uniform, the three casts containing the mild steel samples were mounted onto a Tegra Force-5 polishing unit and ground flat using silicon carbide paper (grade P-300). An ethanol based lubricant was used during the polishing process rather than water to avoid inadvertent corrosion.

Additional hand grinding and cleaning was carried out prior to each experimental run (corrosion measurement or contact angle measurement) using the following procedure. The cast was rinsed with deionised water to remove all residue of the aqueous solution from the previous run. The surface was sanded manually using a grade P-400 silicon carbide abrasive paper to remove any corrosion products. This was followed by abrasion using P-800 paper and ethanol (100% analytical reagent from Chem-supply) as the lubricant. The sample was rotated by approximately 45° after two strokes on the abrasive paper to improve the flatness of the surface. Ethanol was used to remove silicon carbide and epoxy particles present on the steel surface. Any remaining particles were removed using a lint free cleaning tissue (Kimberly Clark Kimwipes). The cast was then rinsed again with ethanol and finally blow dried using nitrogen gas.

2.3 Corrosion Measurements

Corrosion measurements on each sample were performed using a Voltalab PGZ 100 potentiostat and VoltaMaster 4 software. A standard three electrode setup was used with the cast sample (connected by the screw/spring arrangement) acting as the working electrode, a platinum counter electrode and a saturated calomel reference electrode. Linear polarisation resistance (LPR) was used to monitor the corrosion rate on each sample over one hour. The measurement parameters were based on ASTM G59-97 for taking potentiodynamic polarisation resistance measurements: a scan rate of 0.167 mVs^{-1} and an overvoltage of 20 mV. The LPR measurements were conducted in triplicate.

Potentiodynamic measurements were used to characterise the general electrochemical response of the metal in each of the solutions studied. They were conducted immediately after immersion of the electrodes into the test solution. These measurements were based on ASTM G5-94 using a potential sweep rate of 0.167 mVs^{-1} . The change in current with respect to potential was recorded continuously from E_{corr} to +1.6 V as suggested in the standard. The potentiodynamic measurement was stopped if the current density reached 0.1 Acm^{-2} in order to ensure the mild steel did not pit excessively.

2.4 Contact Angle Measurement Using Sessile Drop

The experimental setup shown in Figure 2 was used to capture images of sessile drops on mild steel and measure the contact angle. The setup consisted of a backlight, a sample holder, an Arc Soft webcam fitted with a 70 mm lens to capture side images of the droplet, and a Moticam 3 MP webcam fitted with a 16 mm lens to capture top images of the droplet.

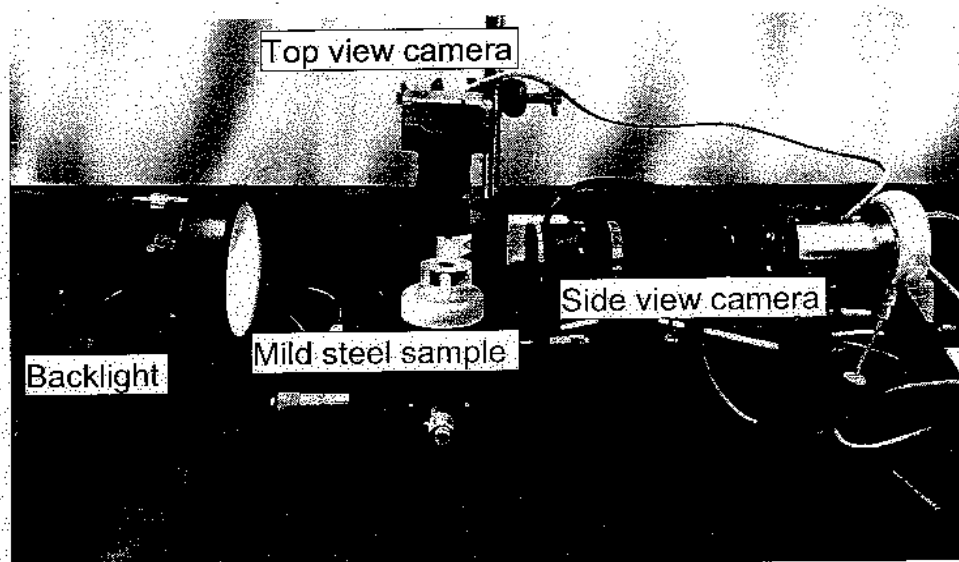


Figure 2 The sessile drop experimental setup.

Droplets of 5 μL for each aqueous solution were placed onto the freshly polished mild steel surface. This was done using a 250 μL microsyringe fitted with a 0.8 x 38 mm Terumo needle tip. Images of the droplet were captured periodically until the droplet evaporated completely. In order to optimize the image analysis for contact angle determination, the silhouette of the droplet was brought into sharp focus.

The contact angle was measured using the ImageJ software and the DropSnake plugin. The software operates by taking a collection of points manually traced around the silhouette of the droplet and fitting a suitable curve to the shape from which the contact angle is obtained. The contact angles measured were reliably determined within 2° .

3. RESULTS AND DISCUSSION

3.1 Corrosion Measurements

The experimentally determined $1/R_p$ determined from the LPR measurements, shown in Figure 3a, indicate the relative corrosion rates of mild steel in the three solutions over an hour. The corrosion rate in H_2SO_4 is about an order of magnitude higher than that in NaCl which is an order of magnitude higher than the corrosion rate in NaOH. Since H_2SO_4 is a strong acid it provides a high concentration of H^+ which accelerates the anodic reaction of Fe to Fe^{2+} . A decaying trend in the corrosion rate of mild steel in H_2SO_4 with respect to time is observed in Figure 3. It can be attributed to the consumption of the reagents (either Fe or H^+) which reduces the rate of the redox reactions.

The corrosion rate of mild steel in NaCl was determined to be lower than in H₂SO₄. The cathodic reaction in NaCl is expected to be dominated by the oxidation of O₂ since the concentration of H⁺ in NaCl is lower than in the acid. Although the presence of Cl⁻ would indicate pitting, time is required for Cl⁻ to weaken the passive film and initiate pitting. Therefore, the corrosion rate of mild steel in NaCl is lower than the corrosion rate in H₂SO₄.

The corrosion rate of mild steel in NaOH was determined to be the lowest. This suggests that OH⁻ assists the passivation of the mild steel surface and hence protect it from corroding. Note that the corrosion rate in NaOH is so low that most of the LPR plots in NaOH (not shown) did not show linearity.

The potentiodynamic polarisation curves, shown in Figure 3b, support the corrosion rate measurements. Mild steel in contact with either H₂SO₄ or NaCl becomes increasingly active as the applied potential becomes more positive. In NaOH the steel tends to passivate with increasing positive potential. This suggests that a protective and adherent oxide film is formed on the mild steel which is consistent with the LPR measurements where a very low corrosion rate was observed.

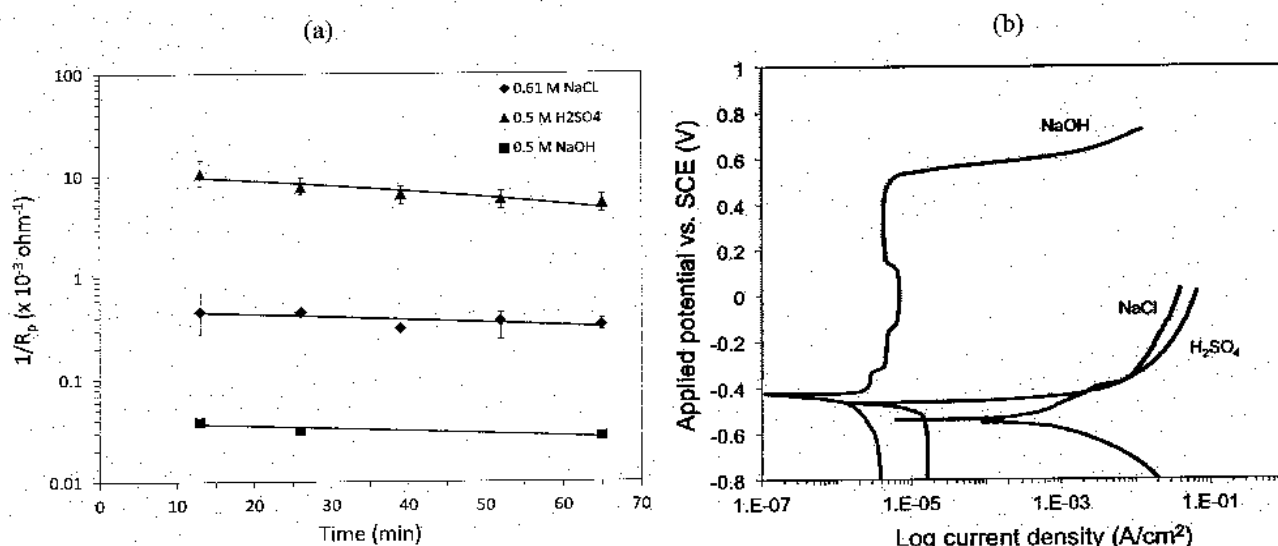


Figure 3 (a) Relative corrosion rate ($1/R_p$) as a function of time measured using LPR and (b) potentiodynamic measurements for mild steel samples immersed in 0.61 M NaCl (blue curve), 0.5 M H₂SO₄ (green curve) and 0.5 M NaOH (red curve).

3.2 Scanning Electron Microscope and Optical Images

A collection of SEM images of the mild steel surface (prepared by abrading with P-800 silicon carbide paper) following contact with each of the solutions are presented in Figures 4 to 6.

3.2.1 0.5 M NaOH Droplet

Figure 4a shows two SEM images of the polished mild steel surface. The inset shows a magnified view ($\times 2000$) of the surface. The abrasive marks on the metal surface due to the mechanical polishing are clearly visible. Holes with sizes of approximately 2 μm and located on the abrasion marks can be seen in the inset. An RMS roughness of 1.1 μm was measured with a stylus profilometer. Figure 4b shows the effect of placing a droplet of NaOH on the mild steel. Minimal spreading was observed, i.e. the deposited droplet did not spread much further than the initial contact area. However, there are two distinct zones within this area: (i) an outer zone (Figure 4c) which was essentially free of deposits apart from around the periphery where the contact line was located during evaporation; and (ii) an inner zone (Figure 4d) filled with crystalline deposits. Spot analysis of the two regions using Energy Dispersive X-ray analysis (EDX) indicated that the deposits consisted of Na, O and Fe while the empty areas consisted of mainly Na and Fe.

3.2.2 0.6 M NaCl Droplet

Figure 5a shows the metal surface after the NaCl droplet has evaporated completely. Again, there was almost no spreading of the droplet. Crystals of 0.2 mm sizes are seen around the periphery where the contact line of the droplet (Figure 5b). Crystals were also present in the interior of the droplet with sizes between 0.1 and 0.2 mm (Figure 5c) although these were sparsely distributed. Note that the pattern formed by the NaCl deposits is opposite to that for the NaOH drop which is densely populated in the centre and sparse at the periphery. EDX analysis of the crystals from the periphery and the interior indicated that they contained Na and Cl only. The areas not covered by crystals consist mainly of Fe and O with small amounts of Na and Cl.

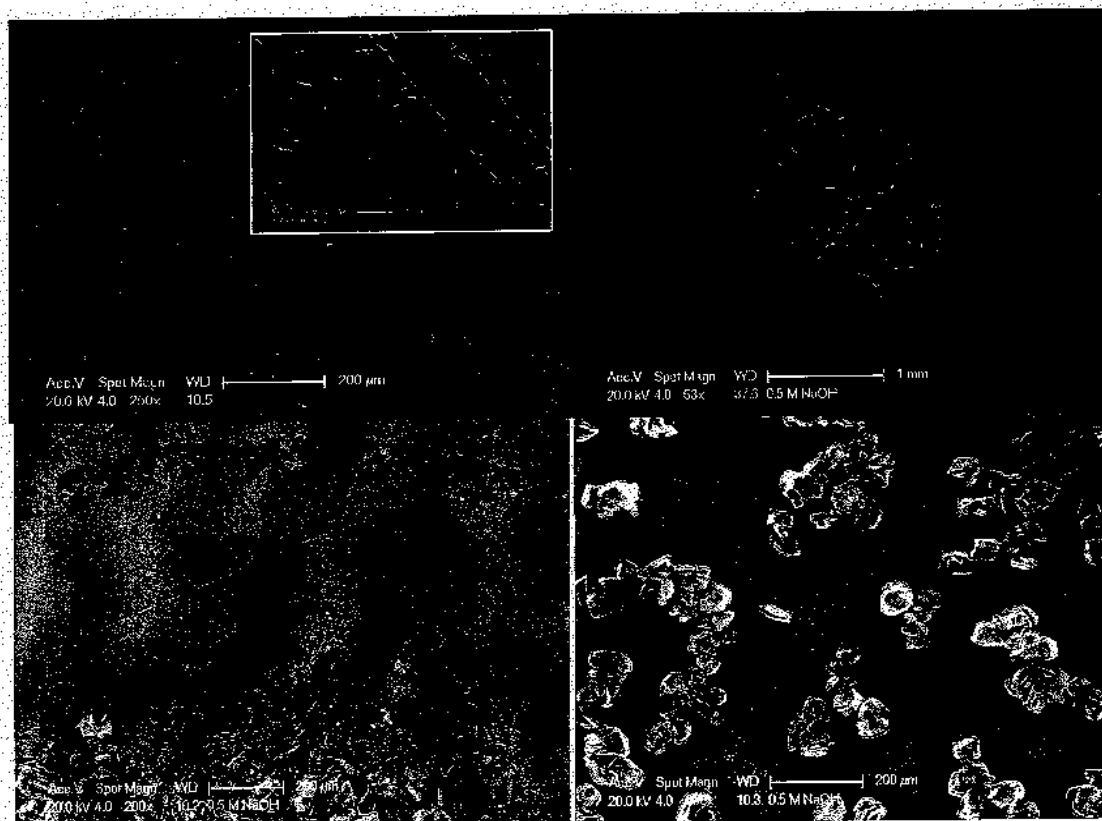


Figure 4 (a) SEM image of the freshly prepared mild steel surface. The inset shows a section of the surface at higher magnification. (b) A low magnification image of the region that was in contact with a NaOH droplet. (c) The periphery of the contact region at increased magnification and (d) the centre of the contact region showing the various crystals present on the surface.

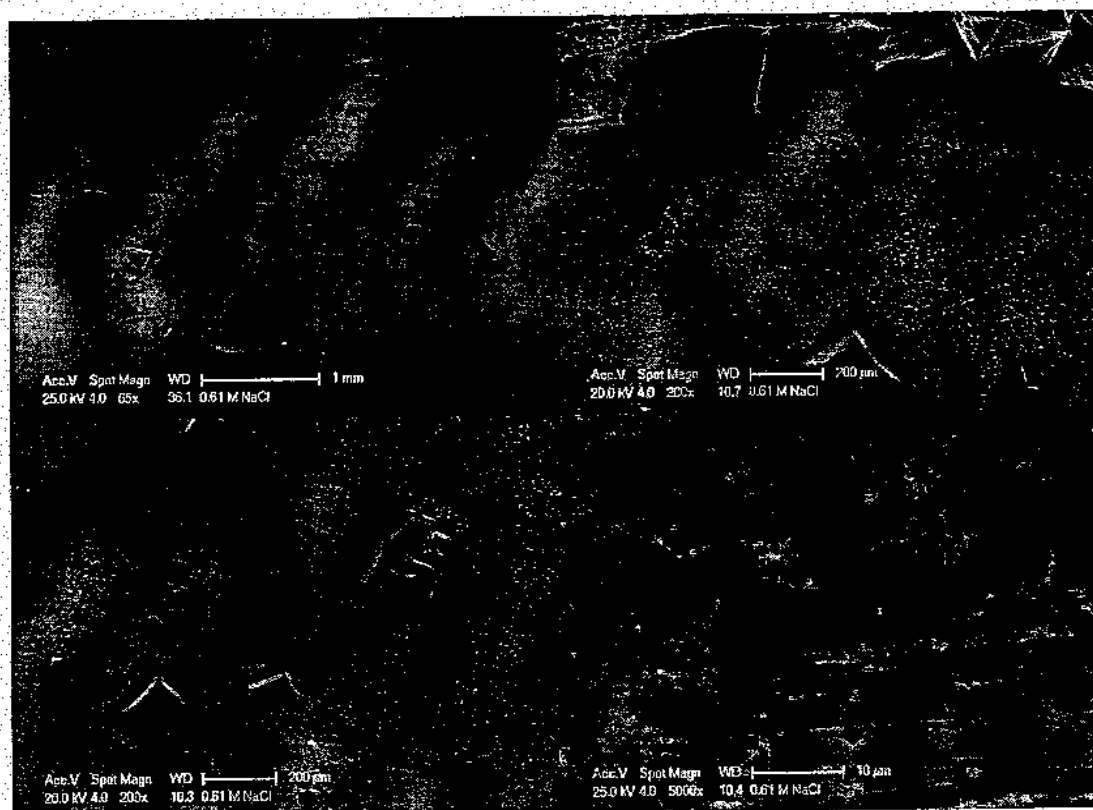


Figure 5 (a) SEM image of the region where a NaCl droplet contacted the mild steel surface. (b) Image of the crystals present at the periphery of the contact region and (c) those in the centre. (d) Small holes – most probably artefacts of the surface preparation rather than due to electrochemical pitting.

The metal surface was also examined for pitting corrosion. No visible large holes were located from the SEM. Only small holes with sizes up to 3 μm (Figure 5d) were found which were of similar sizes to the holes on the initial metal surface. The lack of any visible large pits on the mild steel surface does not mean that pitting is not occurring. Any corrosion products or NaCl crystals formed above the pits would obscure the pits to be seen from the SEM. In addition, pitting is extremely localised and pits usually propagate downwards into the metal and are hard to detect from the surface. However, the lack of visible pitting could indicate that the contact time between the NaCl electrolyte and the steel surface (~ 20 min) is insufficient for pitting to initiate. Usually, pitting propagates at an increased rate once initiated. Corroded samples were cleaned with ethanol and inspected under an optical microscope. These tests did not reveal obvious pitting corrosion. Thus, with respect to the occurrence and the extent of pitting, our experiments were inconclusive.

3.2.3 0.5 M H_2SO_4

Unlike the NaCl and NaOH droplets, the H_2SO_4 droplets exhibit a two-stage, rather asymmetric spreading on mild steel surfaces. Two distinct zones were observed (Figure 6a). The location of the original droplet is indicated by the dotted line (it is not evident in the SEM image but was apparent in optical photographs of the surface). The outer zone was filled with smaller and dense deposits (Figure 6b) which became sparser in the direction away from the initial droplet. In the inner zone where the initial droplet was placed (Figure 6c), larger but sparse deposits were found. EDX analysis indicated that all the deposits had a similar composition of Fe, O and S. The different morphologies of the deposits between the two zones are probably due to different concentrations and time available to crystallise. The liquid in the centre of the droplet persists longer than that at the edges which was also rapidly evaporating during the secondary spreading process. In the inner zone, holes of sizes up to 20 μm (Figure 6d) were found which indicates pitting. Sulphate anions can cause pitting, although not as aggressively as Cl^- .

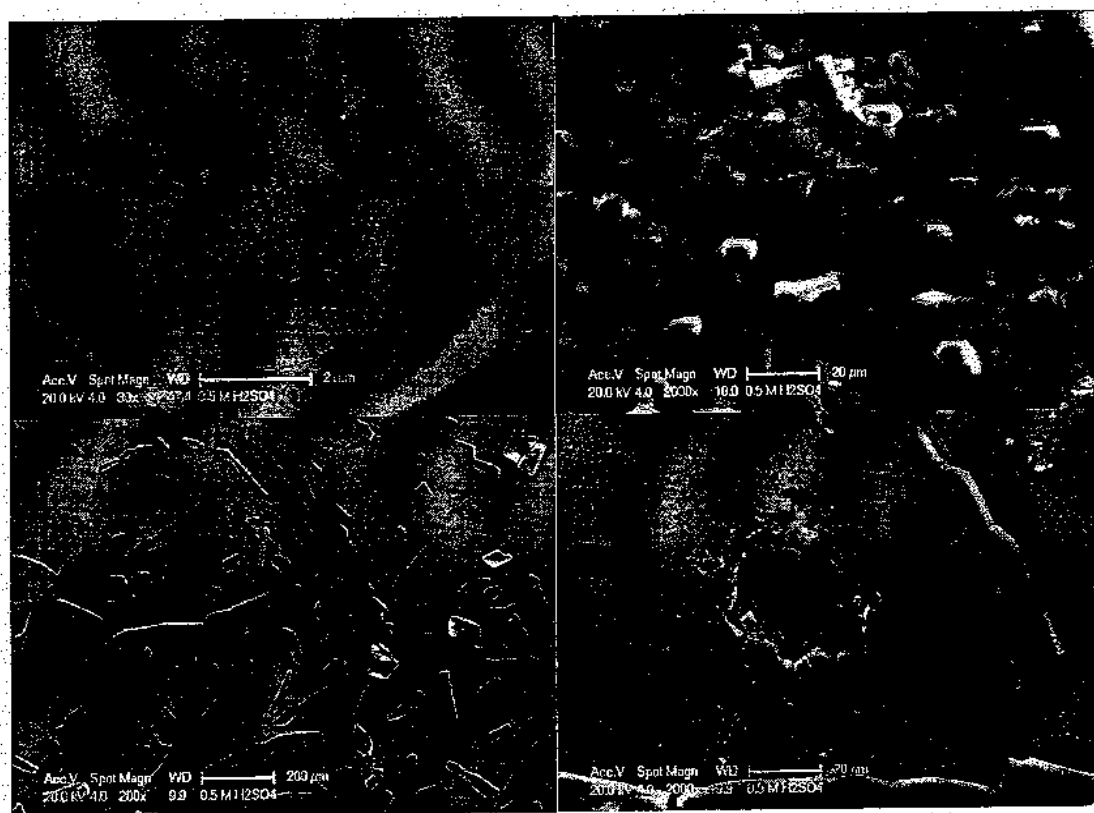


Figure 6 (a) An SEM image of the region where a H_2SO_4 droplet contacted the mild steel surface. The dotted line indicates the original perimeter of the drop when first deposited on the surface. Crystals deposited around in the region beyond the initial drop position once the droplet had spread. (c) the Crystal structure observed within the droplet. (d) An example of pit formation at the surface of the mild steel following exposure to H_2SO_4 .

3.3 Contact Angle Measurements

Figure 7 shows the contact angle as a function of time for NaCl, NaOH and H_2SO_4 droplets on a mild steel surface. In all cases, a decreasing and effectively linear trend is observed.

According to Young's equation the contact angle is determined by the three interfacial tensions. The γ_{SV} should be constant as the metal surface was prepared following the same protocol. The values of γ_{LV} were estimated from literature data (Yizhak, 2010) and for the three aqueous solutions ranged between 73.0 and 74.1 mNm⁻¹. These values are typical for electrolyte solutions and very close to the surface tension of pure water. Therefore the effect on the contact angle is relatively minor. Thus the changes in contact angle (Figure 7) should be attributed entirely to changes in γ_{SL} . According to Young's equation, a contact angle decrease implies that the solid-liquid interfacial tension decreases in time. This makes sense as any spontaneous chemical reaction should decrease the free energy of the system. However, Young's equation is a thermodynamic relation and applies strictly to systems at equilibrium (Adamson & Gast, 1997). Corrosion under the droplet was in all cases significant (Figures 4 to 6) and therefore the contact line was not free to move over the steel surface but stayed pinned. Pinning occurs due to roughness and heterogeneities and is the major cause for contact angle hysteresis (de Gennes et al, 2004). Therefore interpreting the contact angles in Figure 7 with Young's equation is not appropriate.

The following scenario accounts for the observed contact angle changes. After the droplet is deposited it spreads to a certain extent, forming an initial contact angle of about 20-40° (Figure 7). On a really clean metal surface the contact angle of water should be zero but this is never the case as in laboratory atmosphere carbonaceous compounds contaminate quickly any high-energy surface. The original roughness on the steel surface (Figure 4a) pins the contact line and, as corrosion proceeds, the pinning persists (the second stage seen with H₂SO₄ droplets is discussed later). Thus we have an aqueous droplet with a fixed base area (i.e. radius R) subjected to evaporation. For small contact angles, the volume of a spherical cap can be approximated as $V = \theta R^3$. It therefore appears that the contact angle decrease in Figure 7 reflects the gradual evaporation of the droplet. Because of strong pinning, the contact angle observed has little thermodynamic relevance. In this case the contact angle cannot be used to extract energetic information about the solid-liquid interface. It reflects the mass transport (evaporation) during the process but is not directly related to the rate of corrosion.

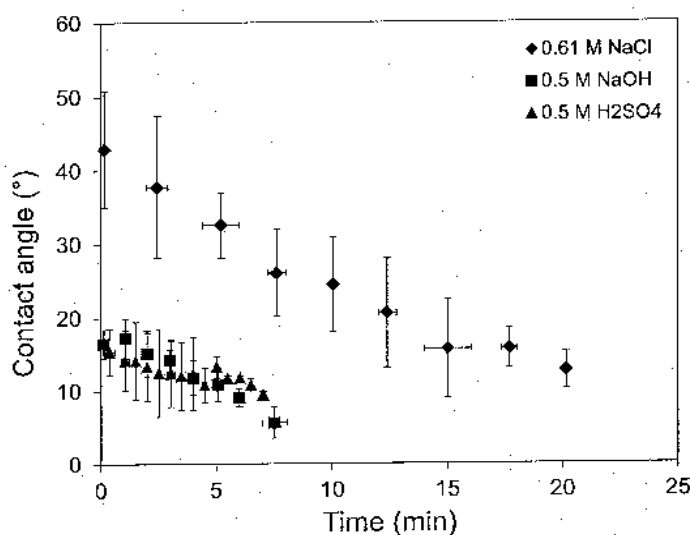


Figure 7 Contact angle versus time of contact for: 0.61 M NaCl (blue diamonds), 0.5 M NaOH (red squares), and 0.5 M H₂SO₄ (green triangles).

3.4. Secondary Spreading of Acidic Droplets

The corrosion chemistry for mild steel is different in the three aqueous environments. However, with H₂SO₄ droplets a secondary spreading stage was observed. A timeline of the droplet evolution is shown in Figure 8. After deposition the droplet assumes a certain noncircular area and corrosion is already happening – gas bubbles can be seen under the droplet (Figure 8a). Gas release becomes more intense (Figure 8b) and then fades away (Figure 8c). Only then the droplet starts spreading beyond the initial contact area (Figure 8d). Evaporation is well advanced and the droplet is visibly drying (Figure 8e) until a completely dry “coffee-stain” trace is obtained (Figure 8f). With both NaOH and NaCl droplets the spreading did not proceed much further than the original contact area. The contrast with H₂SO₄ is seen in Figure 9 where after about 10 min the relative contact area increases very significantly.

A tentative explanation of the behaviour of aqueous droplets on mild steel is outlined as follows. When a droplet is deposited it assumes a certain contact area and forms a rather low contact angle. The wettability of the steel surface is rather good but not perfect because the surface is always contaminated by carbonaceous, and therefore hydrophobic, compounds (a really clean surface can be obtained and studied only under high vacuum). With the neutral (NaCl) droplet corrosion is not intensive (Figure 3) and in time evaporation dictates the outcome. Namely, as the concentration of salt increases crystallization occurs. The largest salt crystals are seen around the periphery of the droplet (Figure 5). This is the

well-known coffee stain effect, where during evaporation internal convection carries material towards the contact line (Deegan, 2000). With the basic droplet (NaOH) the situation is different in that the deposit is mainly located in the central part of the contact area of the original droplet. It appears that, unlike in the NaCl case where transport of the dissolved salt was dominant, in this case the reaction at the metal-solution interface was dominant. With acidic droplets (H_2SO_4), the corrosion reaction dominates the first stage (Figure 8a-c) but then, unlike the neutral and basic droplets, the acidic one spreads further (Figure 8d-f). In accordance with Evans' concept, the periphery of the metal-droplet contact should be more basic than the middle part (Landolt, 2007). This was verified by using an acidic droplet containing a pH indicator. Also gas evolution is less pronounced near the contact line (Figure 8a,b) which indicates acid depletion. We speculate that in the second stage a redistribution of the acid within the drop generates the corrosive power needed to expand the contact area. This is not happening with neutral and basic droplets and their contact area remains within approximately the initial value (Figure 9).

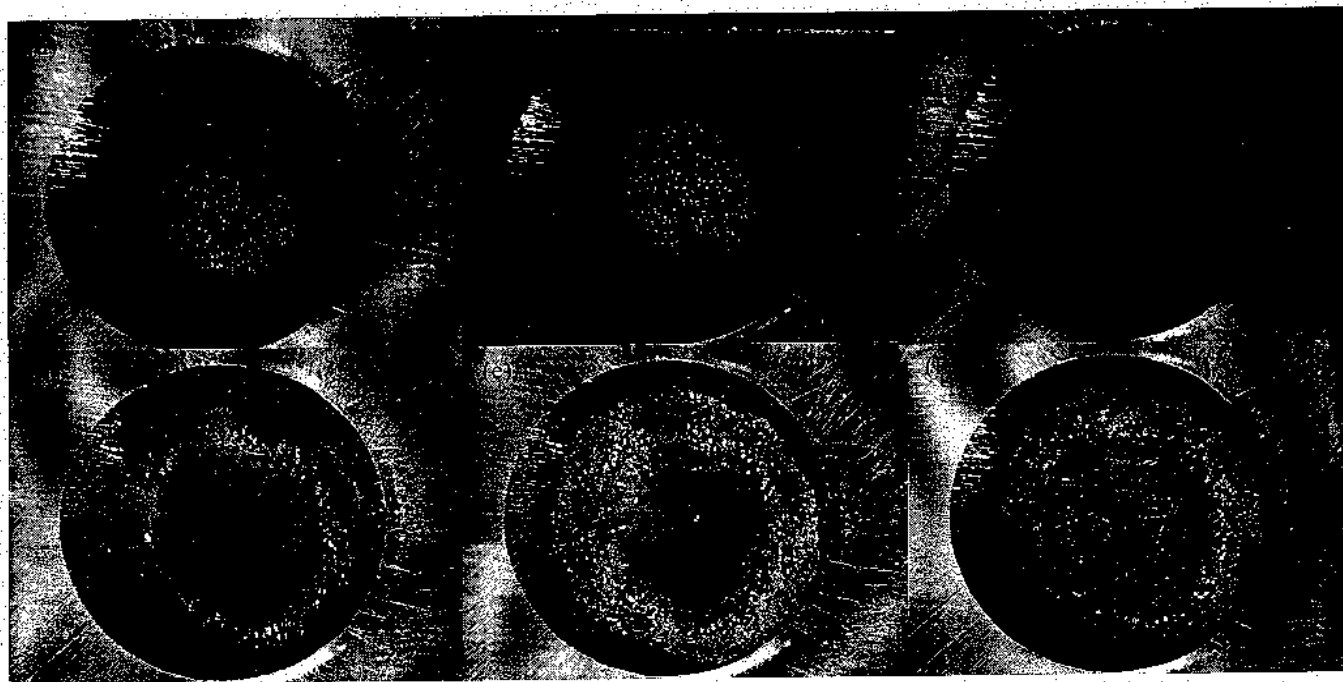


Figure 8 A typical evolution of a H_2SO_4 droplet on a mild steel surface. The acid concentration was 0.25 M and the steel surface was polished using a 3 μm diamond paste. The sequence corresponds to images taken at 0.8, 3.5, 8.8, 11.5, 14.2 and 22.2 min after placing the droplet on the mild steel surface.

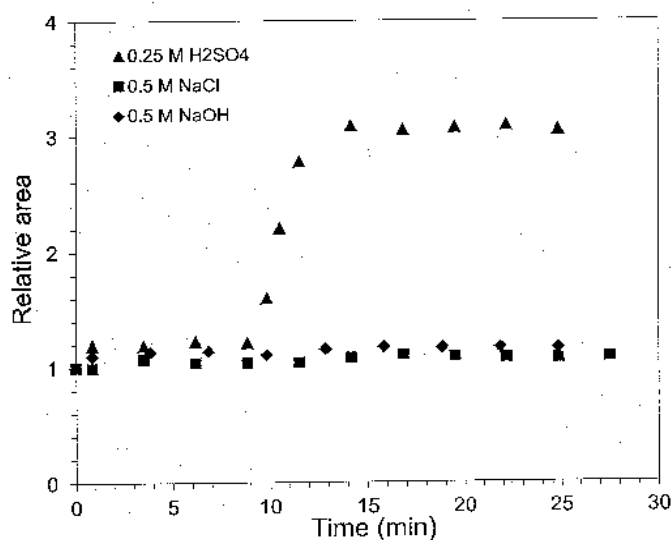


Figure 9 Relative area of the solid-liquid contact as a function of time for droplets of different chemistry placed on mild steel.

We report here detailed observations of the corrosion of mild steel under the influence of small electrolyte droplets. As the conditions change from basic to neutral and acidic, the corrosion rate increases significantly. The spreading is important because it determines the area of contact between the corrosive droplet and the metal substrate. The spreading is minimal with neutral and basic droplets, but a second significant spreading (~300%) is observed with acidic droplets. It appears that corrosion under a discontinuous aqueous phase displays peculiar behaviour due to the limited droplet volume and the confining effect of the contact line. The exact mechanisms are unknown but their knowledge would be of significant benefit in designing tools and structures subjected to spray corrosion.

4. CONCLUSIONS

The following points summarise the outcomes of this study:

1. The LPR corrosion rate of mild steel is highest in 0.5 M H_2SO_4 followed by 0.6 M NaCl and finally 0.5 M NaOH.
2. Potentiodynamic anodic polarisation curves with NaOH showed a wide passive region before a transpassive region. With NaCl and H_2SO_4 only active behaviour was registered.
3. NaCl and NaOH droplets did not spread on the mild steel surface any further than the original contact area. H_2SO_4 droplets spread much further at a later stage.
4. The contact angles measured reflected the evaporation of the droplet but not the energetics of the corrosion reaction.
5. For that reason there is no immediate correlation between wettability and corrosion.
6. The deposits left after complete evaporation of the droplets are of the coffee stain type.
7. For NaCl the deposit is mainly due to crystallisation; for NaOH the passivation reaction changes the pattern; for H_2SO_4 the corrosive reaction induces a second stage spreading.

ACKNOWLEDGMENTS

Financial support from the Australian Research Council is gratefully acknowledged.

5. REFERENCES

- Adamson AW and Gast AP (1997) *Physical Chemistry of Surfaces*, Wiley, New York.
- Ahmad Z (2006) *Principles of Corrosion Engineering and Corrosion Control*, Elsevier, Oxford.
- ASTM (2003) Standard G59-97, Standard Test Method for Conducting Potentiodynamic Polarization Resistance Measurements, ASTM International, West Conshohocken.
- ASTM (1999) Standards G5-94, Standard Reference Test Method for Making Potentiostatic and Potentiodynamic Anodic Polarisation Measurements, ASTM International, West Conshohocken.
- Eustathopoulos N, Drevet B and Nicholas MG (1999) *Wettability at High Temperatures*, Pergamon, Amsterdam.
- Deegan RD (2000) Pattern Formation in Drying Drops, *Phys. Rev. E* 61, 475-485.
- de Gennes PG, Brochard-Wyart F and Quéré D (2004) *Capillarity and Wetting Phenomena: Drops, Bubbles, Pearls, Waves*, Springer, New York.
- Dubuisson E, Lavie P, Dalard F, Caire JP and Szunerits S (2006) Study of the atmospheric corrosion of galvanised steel in a micrometric electrolytic droplet, *Electrochem. Commun.* 8, 911-915.
- Dubuisson E, Lavie P, Dalard F, Caire JP and Szunerits S (2007) Corrosion of galvanised steel under an electrolytic drop, *Corr. Sci.* 49, 910-919.
- Freire L, Nóvoa X, Montemor M, and Carnezim M (2008) Study of passive films formed on mild steel in alkaline media by the application of anodic potentials, *Mater. Chem. Phys.* 114, 962-972.
- Girish K, and Narayan P (2007) Review of non-reactive and reactive wetting of liquids on surface, *Adv. Colloid Interface Sci.* 133, 61-89.

Hastuty S, Nishikata A and Tsuru T (2010) Pitting corrosion of Type 430 stainless steel under chloride solution droplet, *Corr. Sci.* 52, 2035-2043.

King PC, Cole IS, Corrigan PA, Hughes AE and Muster TH (2011) FIB/SEM study of AA2024 corrosion under a seawater drop: Part I, *Corr. Sci.* 53, 1086-1096.

Li S and Hihara LH (2012) In situ Raman spectroscopic identification of rust formation in Evans' droplet experiments, *Electrochem. Commun.* 18, 48-50.

Landolt D (2007) *Corrosion and Surface Chemistry of Metals*, EPFL Press, Lausanne.

Lyon SB (2010) Corrosion of Carbon and Low Alloy Steels in Shreir's Corrosion, Vol. 2 (Eds) Richardson TJA et al. Elsevier, Netherlands.

Muster TH, Bradbury A, Trinchi A, Cole IS, Markley T, Lau D, Dligatch S, Bendavid A and Martin P (2011) The atmospheric corrosion of zinc: The effects of salt concentration, droplet size and droplet shape, *Electrochim. Acta* 56, 1866-1873.







Muster TH, Neufeld AK and Cole IS (2004) The protective nature of passivation films on zinc: wetting and surface energy, *Corr. Sci.* 46, 2337-2354.

Muster TH and Cole IS (2005) The influence of wetting processes on pit formation on 7075-T6 alloys, in 2005 Tri-Service Corrosion Conference, Nov 14-18, Orlando, FL, USA.

Panossian Z, Almeida NL, Sousa RMF, Pimenta GS, and Marques, LBS (2012) Corrosion of carbon steel pipes and tanks by concentrated sulfuric acid: A review, *Corr. Sci.* 58, 1-11.

Yizhak M (2010) Surface Tension of Aqueous Electrolytes and Ions, *J. Chem. Eng. Data* 55, 3641-3644.

6. AUTHOR DETAILS

	L. W. (Aaron) Ng has recently graduated with a degree in Chemical Engineering from The University of Adelaide. He has worked on research projects related to minerals processing, corrosion and wetting. The work presented in this paper was performed as part of his final year project.
	Catherine Fung graduated as a Bachelor of Engineering (Chemical) and Bachelor of Mathematical Science (Applied Mathematics) from the University of Adelaide. She also completed an Honours year at the University of South Australia with a Bachelor of Nano- and Biomaterials Science. She is currently working at the Ian Wark Research Institute as a research assistant.
	Jason Connor is a Senior Research Fellow in Minerals Processing at the Ian Wark Research Institute at the University of South Australia. He has research interests in both applied and fundamental surface science related problems. These include flow accelerated corrosion, plant based corrosion monitoring, minerals processing and surface forces. He had spent a number of years collaborating with alumina industry studying flow accelerated corrosion in spent liquor heat exchangers.
	Yung Ngothai is a Senior Lecturer and Associate Dean (International) in the School of Chemical Engineering at The University of Adelaide. Her research interests range from minerals, materials and biomaterials engineering through to corrosion and scaling in geothermal process.
	David Druskovich is an Associate Professor of Chemistry at CQUniversity in Rockhampton Queensland. His research interests include electrochemical corrosion, flow-enhanced corrosion, heat exchanger plant corrosion and training of graduate station scientists/engineers for the power generation industry. He has supervised a number of chemistry and engineering higher degree students at the Process Engineering and Light Metals Centre at the University's Gladstone campus.
	Rossen Sedev (rossen.sedev@unisa.edu.au) has been a full-time researcher at the Ian Wark Research Institute, University of South Australia since 2000. He is a physical chemist with an interest in wettability, including electrowetting and wetting dynamics, interfacial and electrochemical behaviour of ionic liquids, surface forces, surfactants and colloidal systems. He has published over 90 papers which have received 1400 citations. He is a member of the International Association of Colloid & Interface Scientists, German Colloid Society, American Chemical Society, and Royal Society of Chemistry.